Journal of Colloid and Interface Science 421 (2014) 6–13

Contents lists available at ScienceDirect

Journal of Colloid and Interface Science

www.elsevier.com/locate/jcis

Variation of the crystal growth of mesoporous silica nanoparticles and the evaluation to ibuprofen loading and release

N.H.N. Kamarudin [a], A.A. Jalil [a,*], S. Triwahyono [b], V. Artika [a], N.F.M. Salleh [a], A.H. Karim [b], N.F. Jaafar [b], M.R. Sazegar [b], R.R. Mukti [c], B.H. Hameed [d], A. Johari [a]

[a] Institute of Hydrogen Economy, Department of Chemical Engineering, Faculty of Chemical Engineering, Universiti Teknologi Malaysia, 81310 UTM Skudai, Johor, Malaysia
[b] Ibnu Sina Institute for Fundamental Science Studies, Department of Chemistry, Faculty of Science, Universiti Teknologi Malaysia, 81310 UTM Skudai, Johor, Malaysia
[c] Division of Inorganic and Physical Chemistry, Faculty of Mathematics and Natural Science, Institut Teknologi Bandung, Jl Ganesha No. 10, 40132 Bandung, Indonesia
[d] School of Chemical Engineering, Engineering Campus, Universiti Sains Malaysia, 14300 Nibong Tebal, Penang, Malaysia

ARTICLE INFO

Article history:
Received 11 November 2013
Accepted 24 January 2014
Available online 1 February 2014

Keywords:
Mesoporous silica nanoparticles
Microwave
Ibuprofen
pH
Drug delivery

ABSTRACT

Mesoporous silica nanoparticles (MSNs) were synthesized with variable microwave power in the range of 100–450 W, and the resulting enhancement of MSN crystal growth was evaluated for the adsorption and release of ibuprofen. X-ray diffraction (XRD) revealed that the MSN prepared under the highest microwave power (MSN_{450}) produced the most crystallized and prominent mesoporous structure. Enhancement of the crystal growth improved the hexagonal order and range of silica, which led to greater surface area, pore width and pore volume. MSN_{450} exhibited higher ibuprofen adsorption (98.3 mg/g), followed by MSN_{300} (81.3 mg/g) and MSN_{100} (74.1 mg/g), confirming that more crystallized MSN demonstrated higher adsorptivity toward ibuprofen. Significantly, MSN_{450} also contained more hydroxyl groups that provided more adsorption sites. In addition, MSN_{450} exhibited comparable ibuprofen adsorption with conventionally synthesized MSN, indicating the potential of microwave treatment in the synthesis of related porous materials. *In vitro* drug release was also investigated with simulated biological fluids and the kinetics was studied under different pH conditions. MSN_{450} showed the slowest release rate of ibuprofen, followed by MSN_{300} and MSN_{100}. This was due to the wide pore diameter and longer range of silica order of the MSN_{450}. Ibuprofen release from MSN_{450} at pH 5 and 7 was found to obey a zero-order kinetic model, while release at pH 2 followed the Kosmeyer–Peppas model.
© 2014 Elsevier Inc. All rights reserved.

1. Introduction

Mesoporous silica (MS), which combines the unique properties of nanomaterials and mesostructured substances, are especially promising in gas adsorption, sensing, catalysis, and drug delivery due to their pore accessibility and rapid molecular diffusion [1]. Exclusively in drug delivery, mesoporous silica is often used with modification to suit treatment needs. The study of the loading and release of drugs into/from mesoporous silica is in high demand for the development of tissue regeneration, transdermal therapy, and cell regulation due to the biocompatibility of this material [2]. This material is susceptible to a slow hydrolysis process, which is eventually promoted by dissolved oxygen in the blood. Silicon backbone hydrolysis products such as oxyanions of orthosilicic acid are considered to be low toxicity in the human body [3]. In addition, the half-life of these drugs under physiological conditions can be prolonged by their encapsulation within an inert silica network [4].

The traditional synthesis method of mesoporous materials is the hydrothermal route, which uses a certain amount of surfactants, as well as acid or alkali to compose a mixed aqueous preparation. Next, inorganic sources are added and heated to crystallize, followed by filtration, drying, and calcination or extraction to remove the template. Although finely ordered mesoporous materials are obtained, the process is time and energy consuming [5–6]. Heating solids in the conventional system lead to an uneven temperature distribution due to poor heat transfer into the bulk of the material. The outer temperature may be substantially higher than the inner one, because the material itself acts as an insulator.

In these modern days where scientific findings and technology go hand in hand, any improvement to a synthesis technique that saves time in the synthesis of new materials or improves the properties of materials would be extremely beneficial [7]. It is known

* Corresponding author. Fax: +60 7 5536165.
E-mail address: aishah@cheme.utm.my (A.A. Jalil).

http://dx.doi.org/10.1016/j.jcis.2014.01.034
0021-9797/© 2014 Elsevier Inc. All rights reserved.

that hydrothermal synthesis of inorganic materials using microwave (MW) heating promotes nucleation and can reduce the synthesis time and particle size significantly in comparison with the conventional convection heating method [8–10]. Besides, with faster polymerization under MW irradiation, it was also found that the swelling rate of the material was much higher compared to a material prepared by conventional heating. In fact, scanning electron microscopy revealed that the material produced under MW irradiation consisted of evenly distributed pores [11]. Schmink and Leadbeater demonstrated that microwave energy interacts with polar molecules more than non-polar ones; thus, the conversion of electromagnetic energy into kinetic energy is slower than the conversion of kinetic energy into thermal energy. As a result, polar molecules effectively heat the reaction mixture around them [12].

Various aspects of MW applications, especially in mesoporous silica synthesis, have been reported and reviewed. In particular, it has been reported that microwave-assisted synthesis of silica nanoparticles provides an average diameter generally lower than that of conventionally synthesized silica nanospheres [13]. In addition, SBA-15 synthesized under MW conditions was found to exhibit greater stability than that synthesized by the hydrothermal method. For the synthesis of periodic mesoporous organosilica, it was reported that the synthesis time was reduced from 72 h (conventional) to 36 h when the self-assembly process was performed under MW irradiation. The resulting materials exhibited a high surface area, large pore volume and large pore diameters [14]. Significant enhancement of the crystallization rate was observed by increasing the applied MW power, with little effect on the nucleation time, for the synthesis of zeolites, SAPO-11, silicalite, and NaY [15].

Controlled drug delivery systems using mesoporous materials have been reported extensively by several researchers. Recently, Chen et al. reported that 44–69% of low soluble ibuprofen was successfully loaded onto MSN prepared with the binary templates Pluronic F127 and cetyltrimethylammonium bromide (CTAB), with the release of 80–90% of the drug [16]. Furthermore, adsorption of the soluble drug amikacin onto aluminosilicates was obtained at a maximum percentage of 35.6%, and the release percentage was 72.6% [17]. Based on this report, it is a primary concern in drug delivery studies to continuously find the best adsorption and desorption of drugs using tailorable support materials. Therefore, within this context, MW irradiation under different heating power was applied to the synthesis of mesoporous silica nanoparticles (MSNs), with the expectation of a reduction in synthesis time and formation of MSN with enhanced adsorptive properties. The relationship between material crystal growth and crystallinity, surface area, pore size, particle size, and morphology is also discussed. We suggest an approach to the formation of MSN from a mixture of CTAB, water, ethylene glycol, ammonia, and TEOS. Ammonia was chosen as the catalyst and ethylene glycol as the co-solvent because of their polarity, which is higher than that of NaOH and methanol or ethanol which are commonly used to synthesize MSN. The understanding of those parameters provided control of the structural and morphological characteristics of these materials was beneficial for the design of a drug delivery system. The evaluation of MSN crystal growth with varied MW heating power was conducted on the adsorption and release of ibuprofen, a non-steroidal anti-inflammatory drug widely used in the treatment of pain and inflammation in rheumatic disease and other musculoskeletal disorders. Millions of kilograms of ibuprofen are produced and consumed annually by humans [18]; thus, the application of MSN to ibuprofen delivery is crucial and ever-continuing research [19–20]. The kinetics of ibuprofen release is also thoroughly discussed.

2. Experimental

2.1. Materials

Cetyltrimethylammonium bromide (CTAB), ethylene glycol (EG), tetraethylortho-silicate (TEOS), and 3-aminopropyl triethoxysilane (APTES) were purchased from Merck Sdn Bhd, Malaysia. Ammonium hydroxide (NH_4OH) was obtained from QRec, Malaysia. All the chemicals were used as received without further treatment.

2.2. Synthesis of MSN

The MSN samples used in this work were prepared from raw materials as supplied. 2.34 g of CTAB was mixed with 360 mL of distilled water, 60 mL of ethylene glycol, and 14.5 mL of a 25% ammonia solution. The mixture was stirred at the maximum stirring speed at 323 K for 30 min in a water bath. After 30 min, the temperature was increased to 353 K followed by the addition of 2.85 mL of TEOS, and this step was continued for 2 h in the water bath to dissolve all the materials. After stirring for another 2 h, the white solution was moved into a beaker and deposited in the microwave oven under heating power settings of 100, 300, and 450 W in 8, 4 and 1 h, respectively. The variation of time was decided according to the complete evaporation of the solvent mixture for the purpose of shorten the drying time before preceded to calcination. Heating was conducted until a sol–gel of the MSN solution was obtained. The resulting product was collected and dried at 383 K overnight before being calcined at 823 K for 3 h [21–23].

2.3. Materials characterization

The crystallinity of the catalysts was measured with a Bruker Advance D8 X-ray powder diffractometer (XRD) with Cu Kα (λ = 1.5418 Å) radiation as the diffracted monochromatic beam at 40 kV and 40 mA. TEM was carried out using a JEOL JEM-2100F microscope. The samples were ultrasonically dispersed in acetone and deposited on an amorphous, porous carbon grid. The surface morphology and surface elemental analysis of the samples were performed using FESEM-EDX (JEOL JSM-6701F) with an accelerating voltage of 15 kV. The samples were coated with platinum by electro-deposition under vacuum prior to analyses [24–27]. Nitrogen physisorption analysis was conducted on a Quantachrome Autosorb-1 at 77 K. Before the measurement, the sample was evacuated at 573 K for 3 h. The nitrogen desorption analysis was used to estimate the pore width. FT-IR (Perkin Elmer Spectrum GX FTIR Spectrometer) was performed using the KBr method with a scan range of 400–4000 cm^{-1}. Before the measurement, the sample was evacuated at 573 K for 3 h [28–30].

2.4. Ibuprofen loading and release measurements

Powdered mesoporous samples were loaded with ibuprofen by soaking them in an ethanol solution of ibuprofen, followed by continuous stirring for 24 h at 310 K. A 1:1 (by weight) ratio of ibuprofen to solid sample was used. Ibuprofen-loaded samples were recovered by filtration, washed with ethanol and dried for 24 h at 313 K. During the process, aliquots of 2 mL were withdrawn at pre-determined time intervals and centrifuged in a Hettich Zentrifugen Micro 120 before being analyzed by a UV–Vis spectrophotometer (Agilent Technologies) to determine the residual concentration of ibuprofen. Each set of experiments was performed three times. The adsorption band of ibuprofen was taken at a maximum wavelength (λ_{max}) of 264 nm.

The ibuprofen release profile was obtained by adding 0.2 g of the drug-impregnated powders to a 200 mL round-bottom flask containing 100 mL of simulated body fluid (SBF) at 310 K under continuous stirring. The drug concentration in the release fluid at different release time points was determined using the UV–Vis spectrophotometer. In each case, 3 mL of the release fluid was taken out for analysis of the drug concentration, and then 3 mL of fresh SBF was added to the release system.

3. Results and discussion

3.1. Crystallinity and morphology

The MSN series was synthesized at 100 W, 300 W, and 450 W of microwave power. Fig. 1 demonstrates the difference in the hexagonal density of MSN_{100}, MSN_{300}, and MSN_{450} in the low 2θ region. The pattern illustrates the reflection of a typical MCM-41 type material, which consists of an ordered hexagonal array of parallel silica tubes and can be indexed assuming a hexagonal unit cell as (100), (110), and (200) [31]. Since the materials were not crystalline at the atomic level, no reflections were observed at higher angles.

A substantial increment of the diffraction peak intensity corresponding to the (100) reflection was observed upon increasing the microwave power from 100 to 450 W, indicating the alteration of the long-range ordering of the mesoporous structure, while the MSN structure was unchanged. Although the appropriate synthesis time was given to all of the MSN for well crystal growth, the MSN prepared under 450 W exhibited higher crystallinity and silica order as compared to 300 W and 100 W. This may be related to the higher instantaneous microwave power delivery and consequently higher microwave electric field at 450 W during synthesis. A similar observation was reported for the synthesis of iron-platinum nanoparticles using variable microwave power, in which the XRD data revealed an increase in the peak intensity upon increasing the microwave power from 120 to 420 W [32]. After increasing microwave power, the degree of hydration of the CTAB chains may also increase and their interaction with silica species in the solution becomes stronger, in combination with the increasing rate of hydrolysis and polymerization of the TEOS source that led to the formation of more ordered silica. This may also be related to the effect of synthesis temperature, wherein the temperature rapidly rose when the microwaves coupled directly with the molecules of the entire reaction mixture, which led to the instantaneous localized superheating of the substance [33]. A less ordered structure of SBA-16 prepared at a lower temperature was reported due to the low degree of Pluronic F127 chain hydration, which resulted in weaker interactions with the silica species [34]. While the microwave power was also further increased up to 500 W but disordered structure was obtained, this may be due to fast drying (30 min) led to the incomplete condensation of TEOS and molecular assembly.

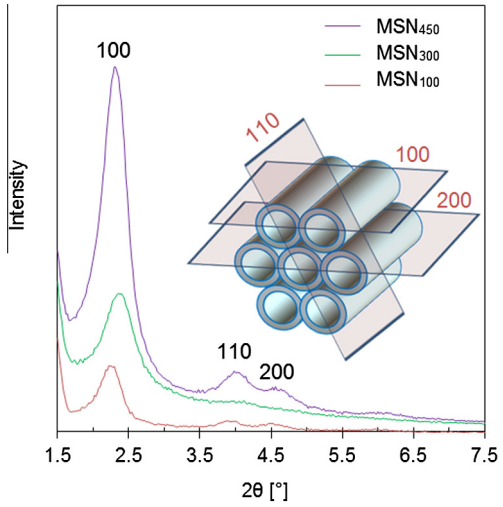

Fig. 1. X-ray diffraction patterns of MSN series.

In fact, the morphologies of mesoporous materials develop after phase separation of the liquid crystal-like phase from the solution and by further growth of solid mesostructure driven by the condensation of the silica species [34]. Thus, the morphology certainly depends on the conditions, and whether nucleation or growth will be predominant over the other, leading to crystals with different sizes and shapes. Figs. 2 and 3 show FESEM and TEM images of the MSNs at different microwave power levels, respectively. Comparing the three MSNs in Fig. 2, spherical particles with smooth surface were observed for the MSN prepared at a microwave power of 450 W; however, irregular particles with a rough surface were formed at a microwave power of 100 W. Moreover, the TEM images in Fig. 3 show clusters of hexagonally-ordered silica nanoparticles approximately 30–45 nm in size. The average particle sizes and ordering of the hexagonal silica were increased with increasing microwave power, since MSN_{450} exhibited more visible long-range silica arrangement. This may be due to the enhanced assembly of parallel CTAB chains upon increasing the microwave power, which resulted in an increased rate of silica hydrolysis; thus, a more ordered silica arrangement was formed compared to the MSN prepared at a low microwave power [35]. This observation is in agreement with the XRD results (Fig. 1), which revealed that an increase in microwave power led to more formation of ordered silica and vice versa. Hence, it can be stated that the crystal growth of MSN was greatly influenced by the microwave power, which resulted in different topologies and particle sizes. It is presumed that these properties will affect MSN behavior regarding ibuprofen adsorption [36]. Indeed, the microwave synthesis of MCM-41 has been reported earlier [37]. In the report, the MCM-41 was synthesized by the composition of synthesis materials of CTAB, TMAOH, TEOS and H_2O, while our in this study, MSN was synthesized using CTAB, ethylene glycol, NH_4OH, TEOS and H_2O. Different particle size was obtained, which is 100 nm for the former, and 30–45 nm for the latter. This may be due to the difference in the composition led to the different crystal growth for both materials.

3.2. Textural parameters

Fig. 4 shows the nitrogen adsorption–desorption isotherms of all MSNs, and Table 1 provides the textural parameters. All MSNs demonstrated a typical type IV isotherm with a significant up-step at a relative pressure of 0.2–0.4, which is associated with the capillary condensation of nitrogen in the channels and also indicates a narrow pore size distribution [38]. The second step at a high relative pressure of P/P_0 = 0.85–0.95 can be attributed to nitrogen condensation that occurs in interparticle pores [39].

Although the typical adsorption steps were clearly identical for all MSNs, MSN_{100} and MSN_{300} showed remarkably less nitrogen adsorption in the region compared to MSN_{450}, suggesting that the surface area and pore structure also differed to some extent with the difference in microwave heating power. However, despite the reduction in the amount of adsorbed nitrogen, the shape of the hysteresis loop remained unchanged, indicating that the pore shape was not significantly altered by the difference in microwave power [40]. During microwave irradiation, MSNs exhibited a sharp temperature increase, which most probably resulted to the differences in the formation of pore structures as this affects the average

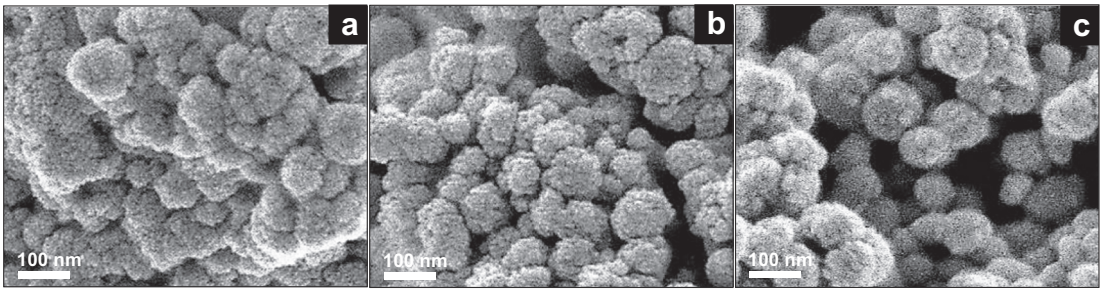

Fig. 2. FESEM image of (a) MSN_{100}; (b) MSN_{300}; and (c) MSN_{450}.

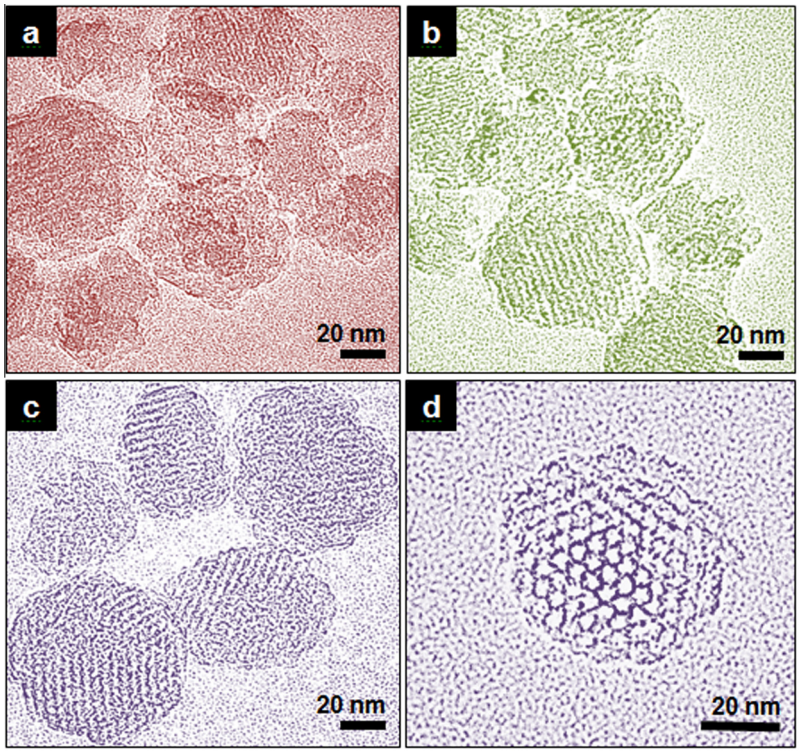

Fig. 3. TEM image of (a) MSN_{100}; (b) MSN_{300}; and (c) MSN_{450} (d) closed up single particle of MSN_{450}.

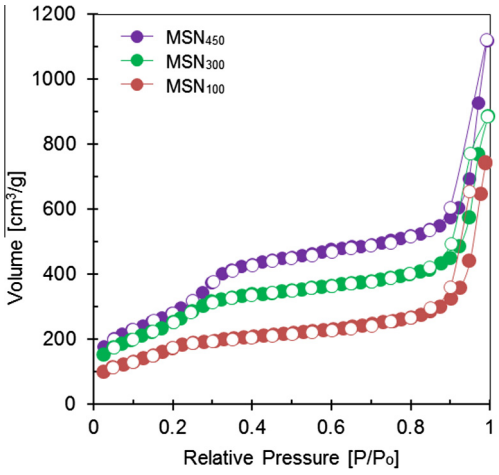

Fig. 4. Nitrogen adsorption and desorption of all MSNs.

pore width. Table 1 presents the distinguishable differences in surface area, total pore volume and pore size of the MSNs. The

Table 1
Textural properties of all MSNs series.

	Surface area (m^2/g)	Pore volume (m^2/g)	Pore width (nm)
MSN_{100}	633	1.16	3.02
MSN_{100}-ibu	308	0.48	2.98
MSN_{300}	728	1.38	3.08
MSN_{300}-ibu	495	0.57	3.07
MSN_{450}	817	1.74	3.13
MSN_{450}-ibu	643	0.71	3.11

surface area was 817 $m^2\,g^{-1}$, 728 $m^2\,g^{-1}$, and 633 $m^2\,g^{-1}$ for MSN_{450}, MSN_{300}, and MSN_{100}, respectively. The difference in microwave power also caused changes in the pore volume and pore width. The pore width and pore volume of MSN_{100}, MSN_{300}, and MSN_{450} were 3.02 nm, 3.08 nm, and 3.13 nm, and 1.16 m^2/g, 1.38 m^2/g, and 1.74 m^2/g, respectively. Apparently, the dissimilarity in the distribution of heat probably resulted in differences in the accumulation of silica, which then led to differences in the surface area and total pore volume. It can be concluded that, at a low microwave power, it is possible to preserve the original mesoporosity created by the surfactant template, while an increase in

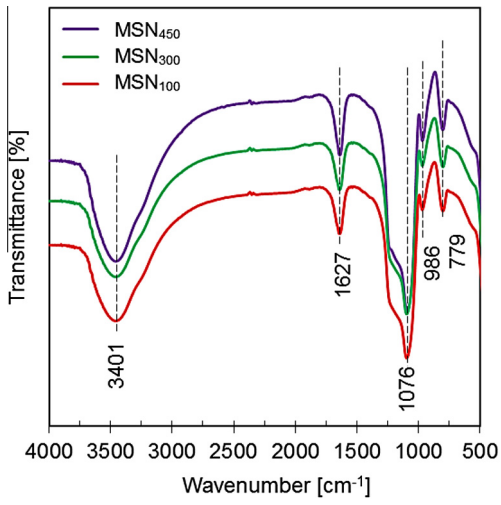

Fig. 5. FT-IR spectra of all MSNs.

microwave irradiation enhances some of the pore structures. This phenomenon most likely occurred due to the type of heating mechanism since microwave heating increases the temperature of the material directly, in contrast to conventional heating [41]. Consequently, the reaction is more rapid as the heating process is almost instantaneous and is concentrated at the points where the microwaves are absorbed. On the contrary, conventional heating is usually a long and relatively slow process and occurs throughout the bulk of the material. In a similar report, increase in the surfactant assembly temperature increased both the framework pore size and the degree of framework cross-linking [42]. A higher assembly temperature was reported to provide a better balance of the hydrolysis and condensation reactions of the siloxane precursors for mesostructure formation as well as an enhancement of the framework pore size. In agreement with our characterization studies, a higher microwave power resulted in the formation of a more highly ordered silica arrangement, as well as a greater surface area and pore size.

3.3. FTIR

FT-IR measurements were performed to identify the structural differences between all the MSNs. The weight of the KBr pellet was measured before and after the powder was collected. This allowed the quantification of the mass of the powder that was responsible for IR absorption. Fig. 5 illustrates the FT-IR spectra of all MSNs in the range of 400–4000 cm^{-1}. All MSNs exhibited IR peaks at the bands attributed to Si–O–Si symmetric stretching (779 cm^{-1}), external Si–OH groups (986 cm^{-1}), Si–O–Si asymmetric stretching (1076 cm^{-1}), water molecules retained by siliceous materials (1627 cm^{-1}), and –OH stretching (3401 cm^{-1}) [43–44]. This result indicates that MSNs retained a siliceous structure despite the differences in microwave power, demonstrating that no major changes occurred in the formation of the framework. It is notable that the relative band of all Si–O–Si vibration modes for MSNat 779 cm^{-1}, 986 cm^{-1}, 1076 cm^{-1} and 1627 cm^{-1} intensified as the microwave power increased, particularly for the band at 1076 cm^{-1}. This suggests that the MSN synthesized at a higher microwave power contained more Si–O–Si bonds in its structure, possibly due to the higher rate of crystal growth at 450 W. In agreement with the XRD and TEM data, this result confirmed the formation of a more substantial silica network in MSN_{450} compared to MSN_{300} and MSN_{100}. A similar result has been reported in the literature, in which an intensified peak of the Si–O–Si bond was observed for silica nanocrystals synthesized at 200 W compared to those synthesized at a lower microwave power [45]. In addition to the abundant Si–O–Si bonds in MSN_{450}, its most intense peak of hydroxyl groups, i.e. the band at 3401 cm^{-1}, also indicated good potential for the efficient adsorption of ibuprofen [23]. Furthermore, the formation of a highly ordered silica arrangement with a high microwave power could also result in greater adsorption of the molecule of interest [36].

3.4. Proposed mechanism

Based on the characterization results, the mechanism for the formation of MSNs using microwaves is proposed. The use of a microwave power of 100 W seemed inadequate since it formed poorly crystalline, irregular mesoporous MSN structures and with a small surface area (Figs. 1–3 and Table 1). Since to the electromagnetic field generated by microwaves affects the enhancement of crystal growth, a low microwave power with a short irradiation time was probably insufficient to provide the homogeneous heating required for optimal crystal growth [46]. The irregularities in the structure were presumed to be a consequence of the formation of "hot spots" at certain locations in the microwave reactor. A similar result was reported regarding the disruption of the ferrite structure due to "hot spots" or areas that induce a localized enhancement in the reaction rate [47]. On the contrary, the use of a microwave power of 450 W generated a more homogeneous and uniform silica order. Although the "hot spots" phenomenon also occurred at 450 W, it is presumed that the strong thermal supply directed the micelles to accumulate faster than at 100 W of microwave power. As a result, the MSN formed at 450 W displayed a more highly ordered structure (Fig. 3d). These differences in MSN characteristics were presumed to affect the adsorption and release pattern of ibuprofen.

3.5. MSN adsorptivity toward ibuprofen

Ibuprofen was used as a model drug to evaluate the adsorptivity and drug storage ability of the synthesized MSNs. It can be seen in Fig. 6 that there was some dissimilarity in the adsorption trends when using MSN synthesized by the conventional method (MSN_{conv}) and by microwave irradiation with variable power. It was thus confirmed that the alterations in MSN crystallinity, morphology, silica arrangement and surface area by varying the microwave power were responsible for the differences in the loading capacity. For the MSN_{conv}, ibuprofen was adsorbed gradually in the first 7 h before complete adsorption was achieved after 10 h [23]. While, MSN_{450} displayed the highest adsorption rate at the

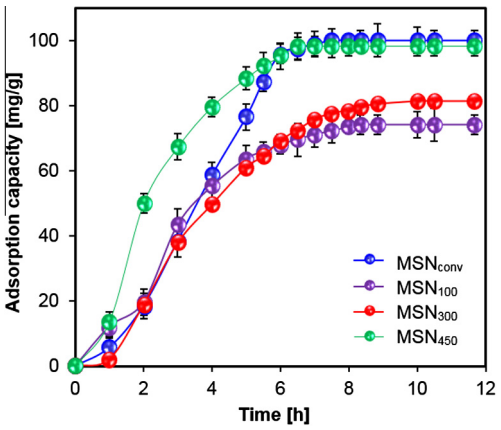

Fig. 6. Adsorption of ibuprofen on MSNs.

first 6 hand almost complete adsorption was achieved with 98.3 mg/g of adsorption capacity after 7 h. The MSN_{300} and MSN_{100} demonstrated almost similar pattern of adsorption with 81.3 and 74.1 mg/g of maximum adsorption capacity, respectively. Although the MSNs had almost the same chemical structure, ibuprofen adsorption increased with an increase in the microwave power used during MSN synthesis. This result implies that the differences in the material properties resulted in variable ibuprofen adsorption behavior.

Based on the characterization by TEM and FESEM, the variation in microwave power led to dissimilar patterns in the material's structure. In parallel with the crystallinity, increasing the microwave power also resulted in the enhancement of hexagonal order and the range of the silica, which led to an increase in surface area, pore width and pore volume. The pore size of all MSNs (3.02–3.13 nm) was accessible to the ibuprofen molecule, which has dimensions of 1.0 × 5.0 nm [48]. The complete adsorption of ibuprofen by MSN_{450} was probably caused by the higher surface area and fewer irregularities in the morphology that resulted in a more accessible surface as compared to MSN_{300} and MSN_{150} [36]. Furthermore, MSN_{450} provided more adsorption sites from abundant hydroxyl groups compared to the other MSNs. This is in correlation with our previous report, which indicated the effect of Si–OH groups in the enhancement of ibuprofen adsorption [23].

In fact, the physicochemical properties of the MSN_{conv} had been reported in our previous work [23]. Comparing the MSN_{conv} and MSN_{450}, TEM and FESEM analyses exhibited that both have similar morphology, topology and particle size (~30–45 nm). Their nitrogen physisorption analysis also displayed similar Type-IV isotherm pattern with a significant up-step at a relative pressure of 0.2–0.4 and 0.85–0.95 which is associated with the capillary condensation of nitrogen in the channels, indicating the narrow pore size distribution. The surface area and pore width of MSN_{conv} were higher than MSN_{450}, while the pore volume of MSN_{450} was slightly higher than MSN_{conv}. These properties may be can explain their similar performance on ibuprofen adsorption.

3.6. Evaluation of MSN on ibuprofen release behavior

It is of great importance to comprehensively understand the drug delivery profiles using *in vitro* simulated body fluid (SBF) before creating a suitable controlled formulation of mesoporous silica materials for use *in vivo*. The concentration of ibuprofen released in SBF as a function of time was determined by monitoring changes in the absorbance by UV–Vis spectroscopy at a wavelength of 264 nm. The release rates are shown in Fig. 7.

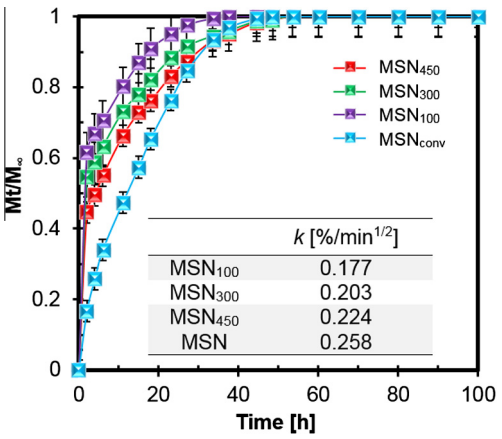

Fig. 7. Release profiles of ibuprofen molecules adsorbed on MSNs.

It can be seen that more than 50 h was necessary to release all of the ibuprofen from the MSNs. The ibuprofen released fastest from MSN_{100}, followed by MSN_{300} and MSN_{450}. MSN_{450} displayed the slowest release rate of ibuprofen (0.177%/$min^{1/2}$) with only 65% of the release percentage of MSN_{300} and MSN_{100} within the same contact time. The release rates of MSN_{300} and MSN_{100} were 0.203%/$min^{1/2}$ and 0.224%/$min^{1/2}$, with 81% and 95% release, respectively. MSN_{100}, with a less ordered silica arrangement, showed the highest release percentage and the fastest drug release rate before equilibrium was reached. Since the pore surface chemistry of the mesoporous silica was quite similar, it is presumed that the difference in drug delivery behavior may be reasonably attributed to the pore diameter and hydroxyl group coverage of the MSN structure (Table 1). In fact, a similar pore diameter and drug molecule size allows for sustained release owing to the size confinement effect; thus, the loaded drug can be released at a relatively high rate when the pore size of the MSN is much larger than the size of the drug molecule [49]. On the contrary, MSN_{450}, which had the largest pore diameter, did not exhibit the fastest release rate. This observation demonstrated the presence of diffusion process constraints during the release process, probably influenced by the pathway (the channel length of silica) of mesoporous silica, as discussed in the XRD characterization. The long ordered channels of MSN_{450} retained ibuprofen molecules, rendering the rapid release of drug molecules from the surface unfavorable. In comparison, the MSN_{conv} exhibited slower release rate of ibuprofen (0.258%/$min^{1/2}$) than the microwave-synthesized MSNs, this may be due to its higher surface area with higher number of silanol groups inhibited the fast release of ibuprofen. In a similar report, fast ibuprofen release was observed with MCM-41, which was characterized by a short channel length [50]. Hence, the length of the pathway is one of the most important factors when investigating drug delivery behavior, in addition to other factors such as the pore size, surface chemistry, and pore geometry of mesoporous silica. In parallel, the greater amount of hydroxyl groups on MSN_{450} could also hold more ibuprofen molecules, resulting to slower release as compared to the other samples.

The phenomenon of the adsorption and release of ibuprofen molecules is proposed according to the XRD, FESEM, and TEM results. Increasing the microwave power was found to form enhanced hexagonal order and range of silica, which led to a greater surface area, pore width and pore volume. After the evaluation of all the MSNs for the adsorption of ibuprofen, MSN_{450} showed a comparable adsorption percentage of ibuprofen to that of conventional MSN, followed by MSN_{300} and MSN_{100}. A greater surface area, fewer irregularities in the morphology and a better silica arrangement were found to improve ibuprofen adsorption.

3.7. Effect of pH

Ibuprofen release from all MSN_{450} was analyzed in a dissolution medium simulating the transition from an acidic to a neutral environment in the human gastrointestinal tract. In oral delivery, ibuprofen is known to be absorbed mainly in the stomach and proximal intestine where the pK_a value is ~4.4. The pH in the human body changes from 1–2 in the stomach body to 5–7 in the antrum, and 7–8 in the proximal intestine [51]. Thus, the release experiments were performed at pH values of 2, 5, and 7 using MSN_{450}. The release profiles are shown in Fig. 8.

The release percentage from MSN_{450} was different under the studied conditions. At pH 2, ibuprofen release from MSN_{450} was very slow, i.e. 26%, while 50% and 95% of the ibuprofen was released at pH 5 and pH 7, respectively. From these result, it can be seen that the ibuprofen molecules exhibited the fastest release in basic rather than acidic medium. At pH 7 (pH > pK_a), most of the drug was ionized and less was retained in the stationary phase[18].

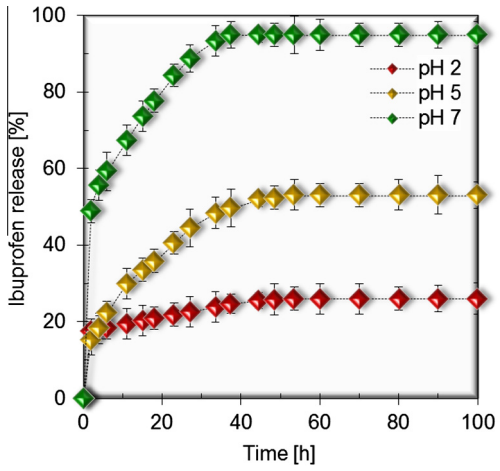

Fig. 8. Release profile of ibuprofen from MSN_{450} in different pH.

Ibuprofen starts to ionize at pH 5 ($pK_a \sim 4.4$) and possibly develops some solute–solute interactions. On the contrary, ibuprofen molecules at pH 2 are more stable and not ionized ($pH < pK_a$) compared to pH 5 and pH 7; this may be due to the abundance of protons under the former conditions. Therefore, the higher solubility of ibuprofen at pH 7 leads to faster release from the MSN_{450}. In addition, the surface of the MSN_{450} particles remained negatively charged at pH 7, and thus repulsed the anionic carboxylic acid group of ibuprofen and led to a higher release rate [52].

In order to investigate the mechanism of ibuprofen release from MSN_{450}, the correlation of kinetic curves was described by zero-order models, which are highly demanded in controlled release systems since this is a long-term and stable process. The ideal delivery of a drug would follow zero-order kinetics, wherein blood levels of the drug would remain constant throughout the delivery period [53]. The release mechanism based on zero-order kinetics was based on drugs that are not chemically bonded to the silica framework (simply entrapped in the mesostructure, as in the case of MSN) [2]. This model fit well with the data on ibuprofen release with correlation coefficients (R^2) of 0.980, 0.999, and 0.987 for pH 2, pH 5, and pH 7, respectively (Table 2). At pH 5, 50% of ibuprofen is ionized and some solute–solute interactions may develop, while some molecules are not in a stationary state. At pH 7, most of the drug exists in its ionized form and the surface of the MSN particles becomes more negatively charged. The negatively charged ibuprofen undergoes strong electrostatic repulsion with the negatively charged MSN_{450}, and thus the release rate is increased at higher pH.

The Korsmeyer–Peppas equation is used to evaluate the release of drugs when the release mechanism is not known or when more than one release phenomena may be involved [54]. This model allows for the *simultaneous* consideration of the diffusion of water into the device and the drug out of the system. In the Korsmeyer–Peppas model, the n value is the diffusional exponent and represents the mechanism of drug release for cylindrically-shaped matrices. When n is equal to 0.5 ($n \approx 0.5$), the drug diffuses with a quasi-Fickian diffusion mechanism from a matrix tablet. Values of n greater than 0.5 and lesser than 1 ($1 > n > 0.5$) indicate nearly zero-order, anomalous, or non-Fickian transport mechanisms, where Fickian is drug transport through the pores of tablet matrix, zero-order indicates a drug transport mechanism through the erosion of the silica wall, and the anomalous mechanism occurs through a combined effect of diffusion and erosion [55].

Next, the release data at pH 2 were fitted to the Korsmeyer–Peppas model. Data obtained from *in vitro* drug release studies were plotted as the log cumulative percentage drug release versus log time and the linearity of the regression line was determined by the R^2 value (Table 2). The R^2 values were 0.993, 0.922, and 0.984 for pH 2, pH 5, and pH 7, respectively. From these data, the Korsmeyer–Peppas model was found to fit well to the release mechanism at pH 2. Moreover, the n values were 0.4200, 0.0938, and 0.2272 for pH 2, 5, and 7, respectively, indicating the appropriateness of this model at pH 2. Ibuprofen molecules are not ionized at pH 2 ($pH < pK_a$) and therefore most of the ibuprofen molecules are in a stationary phase. The release follows the Fickian diffusion mechanism in which the drug is transported through the pores of the silica matrix. Hydrogen bonding between ibuprofen and MSN_{450} is relatively weak, so the diffusion of ibuprofen molecules through the channels will be the controlling step, such that the release process follows Fick's diffusion mechanism.

Table 2
Results of model fitting of ibuprofen release from MSN_{450}.

		pH 2	pH 5	pH 7
Zero order	K_o	5.83	0.206	1.65
	R^2	0.980	0.999	0.986
Korsmeyer–Peppas	n	0.420	0.0938	0.227
	K_k	0.116	0.0356	0.0899
	R^2	0.993	0.922	0.984

4. Conclusion

The enhancement of crystal growth was observed in the formation of mesoporous silica nanoparticles synthesized with variable microwave power in the range of 100–450 W. The use of low heating power (100 W) resulted in low crystallinity, an irregular mesoporous structure and a low surface area of MSN_{100}, which on the contrary, highest heating power produced more crystallized and better silica arrangement. In relation to the adsorption properties, the loading of ibuprofen onto MSNs was conducted in comparison with conventional MSN. Both MSN and MSN_{450} exhibited almost comparable ibuprofen adsorption. However, by the variation of MW heating power, MSN_{450} demonstrated the highest ibuprofen adsorption (98.3 mg/g), followed by MSN_{300} (81.3 mg/g) and MSN_{100} (74.1 mg/g), confirming that the difference in the material properties was a contributing factor in ibuprofen adsorption. By exhibiting the most crystallized structure, complete adsorption of ibuprofen by MSN_{450} was probably caused by the higher surface area and fewer irregularities in its morphology that resulted in a more accessible surface compared to MSN_{300} and MSN_{150}. MSN_{450} also contained significantly more hydroxyl groups that could provide more adsorption sites. In accordance, MSN_{450} showed the slowest release rate of adsorption due to its wide pore diameter and long range of silica order. Ibuprofen release from MSN_{450} at pH 5 and 7 obeyed zero-order kinetic models, while at pH 2 release followed the Kosmeyer–Peppas kinetic model.

Acknowledgments

The authors are grateful for the financial support by the Research University Grant from Universiti Teknologi Malaysia (Grant No. 02H76), the awards of MyPhD Scholarship (Nur Hidayatul Nazirah Kamarudin) from Ministry of Higher Education, Malaysia, and to the Hitachi Scholarship Foundation for their support.

References

[1] S.R. Zhai, C.S. He, D. Wu, Y.H. Sun, J. Non-Cryst. Solids. 353 (2007) 1606–1611.
[2] H.-Y. Lian, Y.-H. Liang, Y. Yamauchi, K.C.W. Wu, J. Phys. Chem. C115 (2011) 6581–6590.
[3] J. Salonen, V.-P. Lehto, Chem. Eng. J. 137 (2008) 162–172.
[4] S. Radin, S. Falaize, M.H. Lee, P. Ducheyne, Biomaterials 23 (2002) 3113–3122.

[5] Q. Yu, J. Hui, P. Wang, B. Xu, J. Zhuang, X. Wang, Nanoscale 4 (2012) 7114–7120.
[6] T. Jiang, W. Shen, Q. Zhao, M. Li, J. Chu, H. Yin, J. Solid State Chem. 181 (2008) 2298–2305.
[7] V.K. Saxena, U. Chandra, Microwave Synthesis: A Physical Concept, Microwave Heating, U. Chandra (Ed.) InTech, 2011.
[8] S.-S. Yoon, W.-J. Son, K. Biswas, W.-S. Ahn, Bull. Korean Chem. Soc. 29 (2008) 609–614.
[9] Y.K. Hwang, J.-S. Chang, Y.-U. Kwon, S.-E. Park, Microporous Mesoporous Mater. 68 (2004) 21–27.
[10] B.L. Newalkar, J. Olanrewaju, S. Komarneni, J. Phys. Chem. B 105 (2001) 8356–8360.
[11] K. Xu, W.D. Zhang, Y.M. Yue, P.X. Wang, J. Appl. Polym. Sci. 98 (2005) 1050–1054.
[12] Jason R. Schmink, Nicholas E. Leadbeater, Org. Biomol. Chem. 7 (2009) 3842–3846.
[13] A.B. Corradi, F. Bondioli, A.M. Ferrari, B. Focher, C. Leonelli, Powder Technol. 167 (2006) 45–48.
[14] B.E. Grabicka, M. Jaroniec, Microporous Mesoporous Mater. 119 (2009) 144–149.
[15] M. Gharibeh, G.A. Tompsett, K.S. Yngvesson, W.C. Conner, J. Phys. Chem. B113 (2009) 8930–8940.
[16] Z. Chen, X. Li, H. He, Z. Ren, Y. Liu, J. Wang, Z. Li, G. Shen, G. Han, Colloids Surf. B: Biointer. 95 (2012) 274–278.
[17] S. Nastase, L. Bajenaru, C. Matei, R.A. Mitran, D. Berger, Microporous Mesoporous Mater. 182 (2013) 32–39.
[18] T. Ahmad, B. Srihari, B. Alresheedi, N.M. Gowda, Int. J. Appl. Sci. Technol. 2 (2012) 49–56.
[19] A.A. Jalil, N. Kurono, M. Tokuda, Synthesis 18 (2002) 2681–2686.
[20] A.A. Jalil, N. Kurono, M. Tokuda, Synlett 12 (2001) 1944–1946.
[21] R.R. Mukti, H. Hirahara, A. Sugawara, A. Shimojima, T. Okubo, Langmuir 26 (4) (2009) 2731–2735.
[22] A.H. Karim, A.A. Jalil, S. Triwahyono, S.M. Sidik, N.H.N. Kamarudin, R. Jusoh, N.W.C. Jusoh, B.H. Hameed, J Colloid Interface Sci. 386 (2012) 307–314.
[23] N.H.N. Kamarudin, A.A. Jalil, S. Triwahyono, N.F.M. Salleh, A.H. Karim, R.R. Mukti, B.H. Hameed, A. Ahmad, Microporous Mesoporous Mater. 180 (2013) 235–241.
[24] N. Sapawe, A.A. Jalil, S. Triwahyono, M.I.A. Shah, R. Jusoh, N.F.M. Salleh, B.H. Hameed, A.H. Karim, Chem. Eng. J. 229 (2013) 388–398.
[25] A.A. Jalil, M.A.H. Satar, S. Triwahyono, H.D. Setiabudi, N.H.N. Kamarudin, N.F. Jaafar, N. Sapawe, R. Ahamad, J. Electroanal. Chem. 70 (2013) 50–58.
[26] A.A. Jalil, S. Triwahyono, M.R. Yaakob, Z.Z.A. Azmi, N. Sapawe, N.H.N. Kamarudin, H.D. Setiabudi, N.F. Jaafar, S.M. Sidik, S.H. Adam, B.H. Hameed, Bioresour. Technol. 120 (2012) 218–224.
[27] M.A.Z. Abidin, A.A. Jalil, S. Triwahyono, S.H. Adam, N.H.N. Kamarudin, Biochem. Eng. J. 54 (2011) 124–131.
[28] N.H.N. Kamarudin, A.A. Jalil, S. Triwahyono, R.R. Mukti, M.A.A. Aziz, H.D. Setiabudi, M.N.M. Muhid, H. Halimaton, Appl. Catal. A: Gen. 431–432 (2012) 104–112.
[29] N.F. Jaafar, A.A. Jalil, S. Triwahyono, M.N.M. Muhid, N. Sapawe, M.A.H. Satar, H. Asaari, Chem. Eng. J. 191 (2012) 112–122.
[30] N. Sapawe, A.A. Jalil, S. Triwahyono, R.N.R.A. Sah, N.W.C. Jusoh, N.H.H. Hairom, J. Efendi, Appl. Catal. A: Gen. 456 (2013) 144–158.
[31] T. Heikkila, H.A. Santos, N. Kumar, D.Y. Murzin, J. Salonen, T. Laaksonen, L. Peltonen, J. Hirvonen, V.-P. Lehto, Eur. J. Pharm. Biopharm. 74 (2010) 483–494.
[32] S. Acharya, K. Singh, J. Microwave Power Electromag. Energy. 45 (2011) 63–69.
[33] B.L. Hayes, Microwave Synthesis: Chemistry at the Speed of Light. CEM Publishing: Matthews, NC, 2002.
[34] C. Yu, J. Fan, B. Tian, D. Zhao, Chem. Mater. 16 (2004) 889–898.
[35] M.A. Ballem, J.M. Córdoba, M. Odén, Microporous Mesoporous Mater. 129 (2010) 106–111.
[36] B. Chen, Z. Wang, G. Quan, X. Peng, X. Pan, R. Wang, Y. Xu, G. Li, C. Wu, Int. J. Nanomedicine 7 (2012) 199–209.
[37] C.-G. Wut, T. Bein, Chem. Commun. (1996) 925–926.
[38] A. Szegedi, M. Popova, I. Goshev, J. Mihaly, J. Solid State Chem. 184 (2011) 1201–1207.
[39] J. Wang, J. Sugawara-Narutaki, A. Shimojima, T. Okubo, J. Colloid Interface Sci. 385 (2012) 41–47.
[40] L. Zhang, M. Mi, B. Li, Y. Dong, Res. J. Appl. Sci. Eng. Technol. 5 (2013) 1791–1795.
[41] J.A. Menéndez, E.M. Menéndez, A. Garcia, J.B. Parra, J.J. Pis, J. Microwave Power Electromag. Energy 34 (1999) 137–143.
[42] Y. Mori, T.J. Pinnavaia, Chem. Mater. 13 (2001) 2173–2178.
[43] X. Du, J. He, J. Colloid Interface Sci. 345 (2010) 269–277.
[44] S.M. Sidik, A.A. Jalil, S. Triwahyono, S.H. Adam, M.A.H. Satar, B.H. Hameed, Chem. Eng. J. 203 (2012) 9–18.
[45] O. Yasar-Inceoglu, T. Lopez, E. Farshihagro, L. Mangolini, Nanotechnology 23 (2012) 255604.
[46] H. Cheng, J. Cheng, Y. Zhang, Q.M. Wang, J. Crystal. Growth 299 (2007) 34–40.
[47] D. Stuerga, P. Gaillardand, Tetrahedron 52 (1996) 5505–5510.
[48] S. Kapoor, R. Hegde, A.J. Bhattacharyya, J. Control Rel. 140 (2009) 34–39.
[49] F. Qu, G. Zhu, H. Lin, W. Zhang, J. Sun, S. Li, S. Qiu, J. Solid State Chem. 179 (2006) 2027–2035.
[50] F. Qu, G. Zhu, H. Lin, J. Sun, D. Zhang, S. Li, S. Qiu, Eur. J. Inorg. Chem. 19 (2006) 3943–3947.
[51] M. Vallet-Regi, A. Rámila, R.P. del Real, J. Pérez-Pariente, Chem. Mater. 13 (2001) 308–311.
[52] I. Tanis, K. Karatasos, J. Phys. Chem. B 113 (2009) 10984–10993.
[53] G. Singhvi, M. Singh, Int. J. Pharm. Stud. Res. (2011) 77–84.
[54] P. Ritger, N. Peppas, J. Control Rel. 5 (1987) 23–36.
[55] A. Badshah, F. Subhan, K. Rauf, AAPS PharmSciTech 11 (2010) 1397–1404.